Impact of the parallel current in the scrape-off layer of a tokamak on the plasma parameters at the divertor plates

V. Rozhansky[1], E. Kaveeva[1], I. Veselova[1], S. Voskoboynikov[1], D. Coster[2], M. Tendler[3]

[1]*St.Petersburg State Polytechnical University, Polytechnicheskaya 29, St.Petersburg, Russia*
[2]*Max-Planck Institut für Plasmaphysik, EURATOM Association, D-85748 Garching, Germany*
[3]*Alfven Laboratory Royal Institute of Technology, 10044, Stockholm, Sweden*

Introduction

The parallel current in a SOL is a combination of a thermal current and a Pfirsch-Schlueter (PS) current ([1]. The parallel currents at the plates were measured on ASDEX-Upgrade and compared with the simulations performed by B2SOLPS5.0-5.2 transport codes [1]-[2]. At the outer hotter plate the parallel electron velocity associated with the thermal current was some fraction (20-30%) of the ion sound speed. An electron convective heat flow associated with the parallel current is directed from the colder to the hotter divertor and might contribute significantly to the total heat flow to the divertors. As a result account of the parallel heat flux associated with the parallel current should amplify the divertor asymmetry. The level of the effect depends on the initial asymmetry between the divertors.

In the paper the impact of the parallel current is studied for the L-mode of ITER using the B2SOLPS5.2. Previously, ITER simulations were done with the earlier versions of B2SOLPS where the parallel current is absent; see e.g. [3]. It is shown below that the account of the parallel current changes significantly the plasma parameters of the inner divertor. Therefore, in the previous simulations of ITER the temperature at the inner divertor is significantly overestimated and the density is underestimated. In contrast, the change of the parameters of the outer hotter divertor is more modest.

Simple analytical model and estimates

Let us consider simple model for the thermal current with account of finite conductivity. The PS currents are not considered in this Section. Let us assume that the right hand divertor is significantly hotter than the other, Fig.1. Here x is the poloidal coordinate and linear geometry is considered. We assume $T_e = T_i = T$ and $nT(x) = const$. The poloidal current is

$$j_x = j_{\|} b_x = \sigma_{\|} b_x^2 [\frac{1}{en}\frac{\partial (nT)}{\partial x} + \frac{0.71}{e}\frac{\partial T}{\partial x} - \frac{\partial \varphi}{\partial x}]. \quad (1)$$

Here b_x is the ratio of the poloidal to toroidal magnetic field. Since the pressure is constant and j_x is conserved, taking into account that $\sigma_{\|} \sim T^{3/2}$, we have for the potential

$$\varphi = 0.71T/e + A\tilde{x} + B; \qquad d\tilde{x} = dx T_+^{3/2}/T^{3/2}. \tag{2}$$

Here T_+ is the temperature at the hotter plate. If $b_x = b_x(x)$, or for flux expansion, the $\tilde{x}$, should be redefined. At the cold plate potential should be of the order of T_-/e, hence the constant B could be neglected in Eq. (2) provided $T_+ >> T_-$. Expressing the constant A through the potential at the hot plate, one obtains

$$\varphi = (\varphi_+ - 0.71T_+/e)\tilde{x}/\tilde{L}_x + 0.71T_+/e, \qquad \tilde{L}_x = \int_0^{L_x} \frac{T_+^{3/2}}{T^{3/2}} dx \tag{3}$$

The poloidal electron heat flow associated with the current is given by

$$q_j = -2.21 j_x T/e = +2.21\sigma_{\|} b_x^2 \frac{T_+^{3/2}}{T^{3/2}} \frac{\varphi_+ - 0.71T_+/e}{e\tilde{L}_x} T. \tag{4}$$

The conductive poloidal electron heat flow is $q_{\nabla T} = -\kappa b_x^2 \partial T/\partial x$

For upstream it is possible to estimate (T_u is upstream temperature) $\tilde{L}_x = T_+^{3/2}/T^{3/2} L_x$, $\partial T_u/\partial x \sim 2T_u/L_x$. Taking $\varphi_+ \sim 3T_+/e$, one gets for the ratio of the upstream flows

$$|q_j|/|q_{\nabla T}| \sim 1.7T_+/T_u. \tag{5}$$

For example, for $T_+/T_u = 0.2$ one has $|q_j|/|q_{\nabla T}| \sim 1.7T_+/T_u \sim 30\%$. The electron heat flow to the colder divertor is smaller than to the hotter one, so one would expect larger effect for the inner colder divertor. Since the conductive part is transported to the plates both by ions and electrons while the convective flow is transported only by electrons, we have at the hot plate

$$V_{e\|} - c_s/c_s \sim 1.7T_+/T_u\gamma_e + \gamma_i/\gamma_e, \tag{6}$$

where γ_e, γ_i are sheath transmission factors. So the additional electron velocity is comparable with the sound speed as is observed in the experiments and simulations.

Simulations of ITER L-mode

Three ITER L-mode were simulated by the code B2SOLPS5.2. Transport coefficients $\chi_e = \chi_i = 1\ m^2/s,\ D_\perp = 0.3\ m^2/s$ were the same as in the previous ITER simulations [3]. Three values of density and temperatures at the core side of the simulation domain were chosen: $n = 3.75\cdot10^{19};\ 5\cdot10^{19};\ 7\cdot10^{19}\ m^{-3}$, $T_e = T_i = 1.2;\ 0.9;\ 0.7\ keV$ to provide heating power

$P \approx 90 \div 95\ MW$. For each case in the first run all electric fields and currents were switched off which corresponds to the earlier simulations with B2SOLPS4.3 (curves '1'). The second variant corresponds to so called 'no drift case', when $\vec{E} \times \vec{B}$ and diamagnetic drifts were switched off and hence PS currents were absent, but the rest parallel current in the SOL were calculated (curves '2'). This was done to investigate the role of the parallel thermal current in the SOL. In the third type of runs all terms with electric fields and currents were switched on (curves '3'). For the first scenario, a run with impurities was also done (curve'4').

The results for the low density case are shown in Figs.2-7. Switching on the parallel current in the SOL makes the divertor plasma more asymmetric due to the additional electron heat flow from the inner to the outer divertor. Its contribution could be estimated from Fig.1, where the poloidal electron heat flows with and without convective term are plotted. Electron temperature at the inner divertor is more than three times smaller than without the current. Similar change in the ion temperature is observed. The density is changed in the opposite direction and is more than twice larger when the current is switched on. Rise of the separatrix density is observed. At the outer divertor the difference between two cases is more modest. The account of impurities doesn't affect much the plasma parameters (curve '4').

For medium density, Figs.8-9, the qualitative behavior is similar. In both cases there are some further differences associated with drifts which shall be analyzed elsewhere. In the third high density scenario the difference between three runs is rather modest.

Conclusions

The parallel current in the scrape-off layer is responsible for the convective electron energy flow from the colder to the hotter divertor. The convective flow could be comparable with the conductive electron heat flow and could amplify considerably the existing asymmetry in the divertor plasma parameters.

References

[1] V. Rozhansky, E. Kaveeva, S. Voskoboynikov et al Nuclear Fus. **43** 614 (2003)

[2] D. P Coster. et al, Recent developments in tokamak edge physics analysis in Garching \\Proc. 18th IAEA Fusion Energy Conference, Sorrento (2000), paper IAEA-CN-77/EXP5/32David IAEA 2000

[3] A.S. Kukushkin et al Nuclear Fus. **43** (2003) 716

The work was supported by RFBR grant 10-02-00158-a and by Ministry of Education and Science of Russian Federation (contract # 11.G34.31.0001 with SPbSPU and leading scientist G.G.Pavlov)

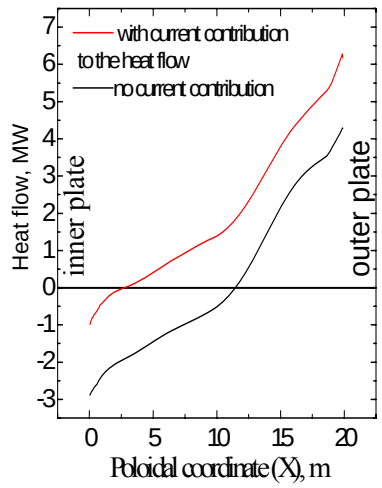

Fig.1

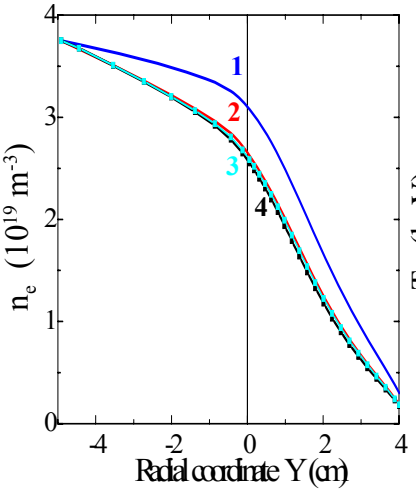

Fig.2

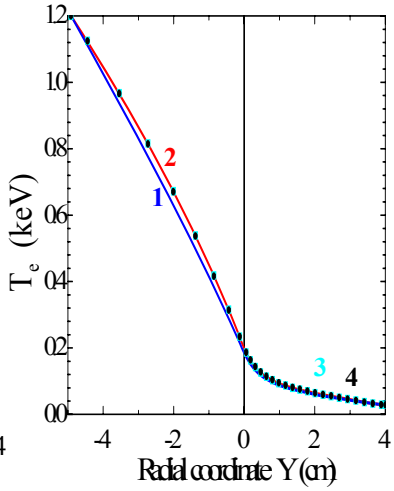

Fig.3

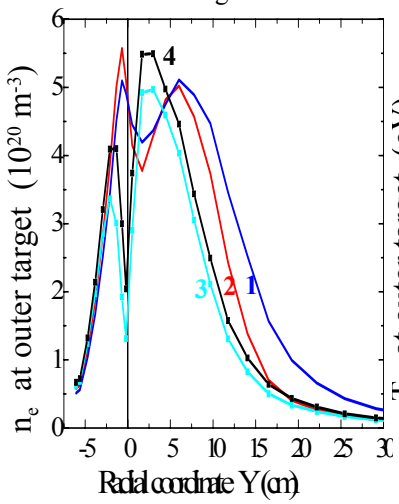

Fig.4

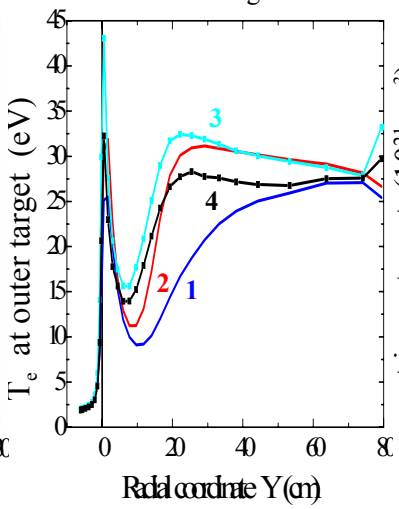

Fig.5

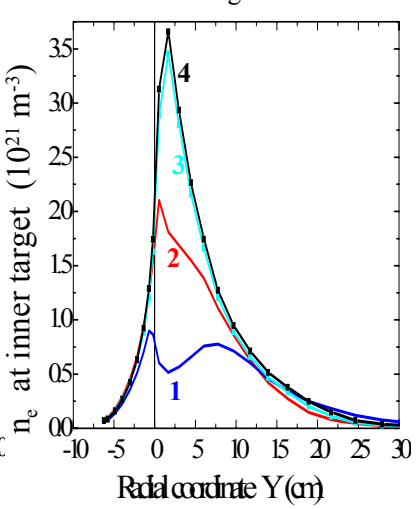

Fig.6

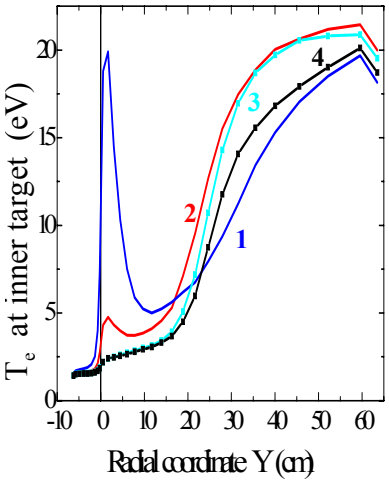

Fig.7

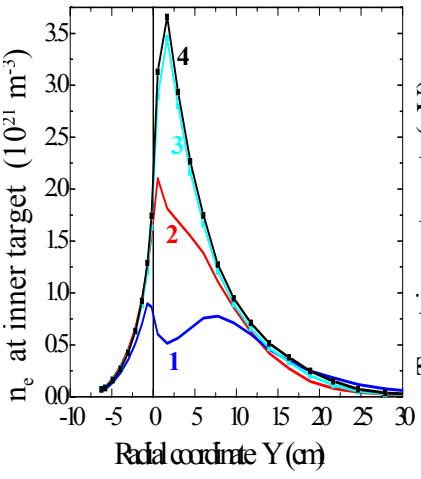

Fig.8

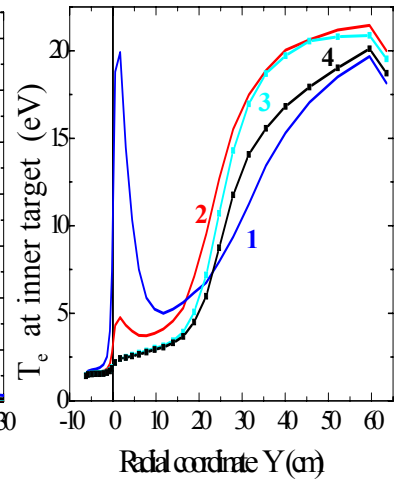

Fig.9

Fig.1. Poloidal electron heat flow between two flux surfaces in SOL. Current contribution to the electron heat flow is switched off (black line) or on (red line). Low density: Fig.2. Density at the outer midplane. Fig.3. Electron temperature at the outer midplane. Fig.4. Density at the outer target. Fig.5. Electron temperature at the outer target. Fig.6. Density at the inner target. Fig.7. Electron temperature at the inner target.

Medium density: Fig.8. Density at the inner target. Fig.9. Electron temperature at the inner target.